analytical chemistry

pubs.acs.org/ac Article

Influence of the Composition of Plasticizer-Free Silicone-Based Ion-Selective Membranes on Signal Stability in Aqueous and Blood Plasma Samples

Brian D. Spindler, Katerina I. Graf, Xin I. N. Dong, Minog Kim, Xin V. Chen, Philippe Bühlmann,* and Andreas Stein*

Cite This: *Anal. Chem.* 2023, 95, 12419−12426 Read Online

ACCESS | Metrics & More | Article Recommendations | Supporting Information

ABSTRACT: Solid-contact ion-selective electrodes (SC-ISEs) in direct long-term contact with physiological samples must be biocompatible and resistant to biofouling, but most wearable SC-ISEs proposed to date contain plasticized poly(vinyl chloride) (PVC) membranes, which have poor biocompatibility. Silicones are a promising alternative to plasticized PVC because of their excellent biocompatibility, but little work has been done to study the relationship between silicone composition and ISE performance. To address this, we prepared and tested K^+ SC-ISEs with colloid-imprinted mesoporous (CIM) carbon as the solid contact and three different condensation-cured silicones: a custom silicone prepared in-house (**Silicone 1**), a commercial silicone (Dow 3140, **Silicone 2**), and a commercial fluorosilicone (Dow 730, **Fluorosilicone 1**). SC-ISEs prepared with each of these polymers and the ionophore valinomycin and added ionic sites exhibited Nernstian responses, excellent selectivities, and signal drifts as low as 3 μV/h in 1 mM KCl solution. All ISEs maintained Nernstian response slopes and had only very slightly worsened selectivities after 41 h exposure to porcine plasma (log $K_{K,Na}$ values of −4.56, −4.58, and −4.49, to −4.04, −4.00, and −3.90 for **Silicone 1**, **Silicone 2**, and **Fluorosilicone 1**, respectively), confirming that these sensors retain the high selectivity that makes them suitable for use in physiological samples. When immersed in porcine plasma, the SC-ISEs exhibited emf drifts that were still fairly low but notably larger than when measurements were performed in pure water. Interestingly, despite the very similar structures of these matrix polymers, SC-ISEs prepared with **Silicone 2** showed lower drift in porcine blood plasma (−55 μV/h, over 41 h) compared to **Silicone 1** (−495 μV/h) or **Fluorosilicone 1** (−297 μV/h).

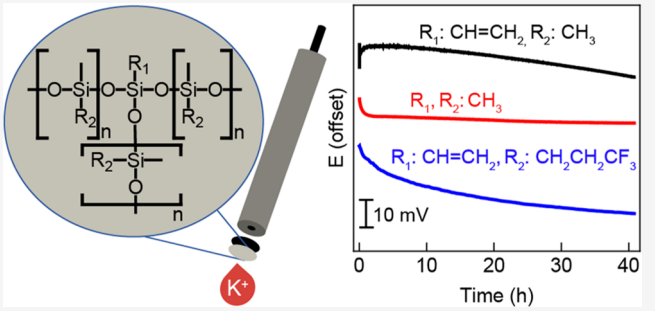

INTRODUCTION

Ion-selective electrodes (ISEs) are widely used in clinical settings for analysis of ion activity in body fluids and in industrial settings for process monitoring.[1−6] Recently, there has also been an increased interest in real-time measurement of ion activity in sweat and interstitial fluid as a noninvasive method to diagnose disease.[7−14] To facilitate this, solid-contact ISEs (SC-ISEs) with solid-contact reference electrodes have been integrated into wearable devices, including patches that can be adhered to the skin.[8,9] For both wearable and implantable ISEs, the ion-selective membrane must be biocompatible. Unfortunately, the majority of ion-selective membranes reported to date comprised plasticized poly(vinyl chloride) (PVC) matrixes, which have poor biocompatibility owing to the large amount of plasticizer required to lower the glass-transition temperature of PVC.[15−17] Furthermore, leaching of plasticizer can limit the lifetime of the sensor.

Several polymers have been studied as alternatives to PVC, including silicones,[18] acrylate- and methacrylate-based polymers,[19,20] and polyurethanes.[21] Among these, silicones have a long history of use in implants owing to their excellent biocompatibility[22] and are a promising alternative to plasticized PVC membranes for wearable and implantable devices. In addition, silicones have low glass-transition temperatures, eliminating the need for a plasticizer. These advantageous properties prompted efforts in the 1980s and 1990s to produce small, biocompatible ion-selective field effect transistors (ISFETs)[23−29] with silicone membranes that could be used to measure real-time ion activities directly in physiological samples like blood. However, these ISFETs never made it past the research stage, presumably due to large drifts caused by the formation of a water layer at the gate oxide

Received: May 12, 2023
Accepted: July 25, 2023
Published: August 8, 2023

https://doi.org/10.1021/acs.analchem.3c02074
Anal. Chem. 2023, 95, 12419−12426

and ion-selective membrane interface.[23] Additionally, silicone has a low polarity, and as a result, many ionophores have poor solubility in silicones. Therefore, a plasticizer is added in some cases (10−30 wt %) into silicone membranes to improve the solubility of the ionophore, which brings some of the same drawbacks mentioned for plasticized PVC membranes.[30−35]

Much of the work using silicone-based ISEs in the literature involves the use of commercially available one-component or two-component silicones, though there are a few reports of silicones prepared specifically for application in ISEs.[28,36−38] Commercially available silicones often have fillers and other additives to improve mechanical properties, which may impact ISE performance.[39,40] Even though silicone-based ISEs have been known for 50 years, the effects of polymer structure, polymerization catalysts, fillers, and curing conditions on long-term stability in biological samples have not been studied in much detail. The only long-term drifts reported to date are, for measurements in aqueous solution, for a conventional silicone-based ISE with valinomycin as ionophore (0.8 μV/h),[41] a Ca^{2+} SC-ISE with ETH1001 as ionophore (200 μV/h),[42] a coated Ag wire K^+ ISE with a fluorosilicone membrane containing 10.5 wt % dioctyl sebacate (DOS) as plasticizer, and a Ag^+ salt redox modifier (10 μV/h),[43] and a K^+ ISE with a silicone membrane coated directly onto a Ag/AgCl electrode (<200 μV/h).[21]

Although there has been a lot of work to characterize the properties of SC-ISEs in aqueous solution (with the exception of long-term drift), little attention has been paid to the effects of continuous long-term exposure of SC-ISEs to real samples like sweat or blood plasma.[44] To investigate the effects of different silicones on the sensor properties, we prepared plasticizer-free K^+ SC-ISEs with colloid-imprinted mesoporous (CIM) carbon as the solid contact[45] using a commercially available silicone and fluorosilicone as well as a silicone prepared in-house. CIM carbon was chosen as the solid-contact material because previous work with plasticized PVC-based ISEs prepared with CIM carbon solid contacts has shown very low long-term potential drift (1.3 μV/h) and insensitivity to interference from light and CO_2. We show here that small changes in silicone composition do not affect the response slope and are all compatible with excellent selectivity even after blood plasma exposure. However, they give rise to some differences in emf drift when measurements are performed in porcine plasma.

EXPERIMENTAL SECTION

Materials. Reagents were purchased from the following sources: Teflon (60 wt % aqueous dispersion), trifluoroacetic acid (99%), valinomycin, potassium tetrakis(*p*-chlorophenyl)-borate (KTpClPB), and hydroxy-terminated poly(dimethylsiloxane) (average molecular weight ∼110 000) from Sigma-Aldrich (St. Louis, MO); vinyltrimethoxysilane (tech-95, VTMOS) and vinyltriisopropenoxysilane (tech-95) from Gelest (Morrisville, PA); Dow Corning 3140 silicone (**Silicone 2**) from Pilots HQ LLC (Waterford, MI); and Dow Corning 730 FS solvent resistant sealant (**Fluorosilicone 1**) from Aircraft Spruce (Corona, CA). The silicone resulting from condensation curing of a precursor solution containing hydroxy-terminated poly(dimethylsiloxane) (PDMS−OH), VTMOS, and trifluoroacetic acid is referred to as **Silicone 1** (see the Supporting Information). Porcine blood was obtained from Medtronic PLC (Fridley, MN). Citrate phosphate dextrose adenine solution (63 mL) was added as an anticoagulant to 450 mL of porcine blood. To obtain plasma, the red blood cells were removed by centrifugation (2000*g*) at room temperature for 20 min.

CIM Carbon Disk Fabrication. A mass of 0.42 g of 60 wt % Teflon dispersion in H_2O was diluted with 4.58 mL of H_2O to 5 wt %. CIM carbon (100 mg) was mixed with 100 μL of the 5 wt % Teflon dispersion with an agate mortar and pestle. The Teflon/CIM carbon/water mixture was mixed manually until the carbon particles stuck together, producing one piece of CIM carbon, which was then pressed into a film (thickness: 137 ± 6 μm) using a roller press. CIM carbon disks were cut out of this film with a hole punch (4.8 mm), and water was removed by heating the disks in a vacuum oven at 120 °C for 18 h.

ISE Fabrication. Precursor solutions for **Silicone 1**-, **Silicone 2**-, and **Fluorosilicone 1**-based K^+ ISEs were prepared as follows. For **Silicone 1**-based K^+ ISEs, 200 mg of PDMS−OH, 10.8 μL of VTMOS, 67 μL of trifluoroacetic acid, 2.0 mg of valinomycin, and 0.45 mg of KTpClPB (50 mol % with respect to valinomycin) were dissolved in 1.0 mL of toluene (see the Supporting Information, Section S1.2 for details on optimization of the precursor solution composition and curing conditions). For **Silicone 2**-based K^+ ISEs, 200 mg of **Silicone 2**, 2.0 mg of valinomycin, and 0.45 mg of KTpClPB were dissolved in 1.0 mL of THF. For **Fluorosilicone 1**-based K^+ ISEs, 200 mg of **Fluorosilicone 1**, 2.0 mg of valinomycin, and 0.45 mg of KTpClPB were dissolved in 1.0 mL of THF.

To prepare the ISEs, a CIM carbon/Teflon disk was placed on top of a graphite/glass electrode and centered (see the Supporting Information, Section S1.4, for details on electrode preparation and Figure S1 for electrode images). Then, 20 μL of solvent (THF for the **Silicone 2** and **Fluorosilicone 1** ISEs and toluene for the **Silicone 1**-based ISEs) was deposited onto the CIM carbon layer. This wetted the CIM carbon and allowed the solvent to infiltrate the pores of the CIM carbon, displacing air from its pores and helping to prevent the formation of air pockets in the ion-selective membrane (ISM) layer while the silicone was curing. When the solvent had evaporated sufficiently to expose the top of the CIM carbon layer (usually 1−2 min after drop-casting for THF and 5 min for toluene), the ISM solution was applied first as a 20 μL portion, followed by four 50 μL portions. The **Silicone 2** and **Fluorosilicone 1** ISEs were cured in air at room temperature for 96 h, whereas the **Silicone 1** ISEs were cured in an oven at 55 °C for 96 h. ISEs from **Batch 1** had a total thickness (membrane + carbon layer) of 820 ± 70, 610 ± 70, and 480 ± 30 μm for **Silicone 1**, **Silicone 2**, and **Fluorosilicone 1**, respectively. We found that the age of **Fluorosilicone 1** affects the response slope and selectivity of the sensors and recommend not to use **Fluorosilicone 1** batches beyond the manufacturer's expiration date. No such effect was observed for **Silicone 2**.

Two batches of SC-ISEs (**Batch 1** and **Batch 2**) were used to evaluate the effects of long-term exposure to porcine plasma. See the Supporting Information, Section S1.9 for the use history of each batch.

For further experimental details, see the Supporting Information.

RESULTS AND DISCUSSION

Silicone Curing. **Silicone 1** is a homemade silicone, whereas **Silicone 2** and **Fluorosilicone 1** are commercial one-component silicones. All three cure to an elastomer upon

https://doi.org/10.1021/acs.analchem.3c02074
Anal. Chem. 2023, 95, 12419−12426

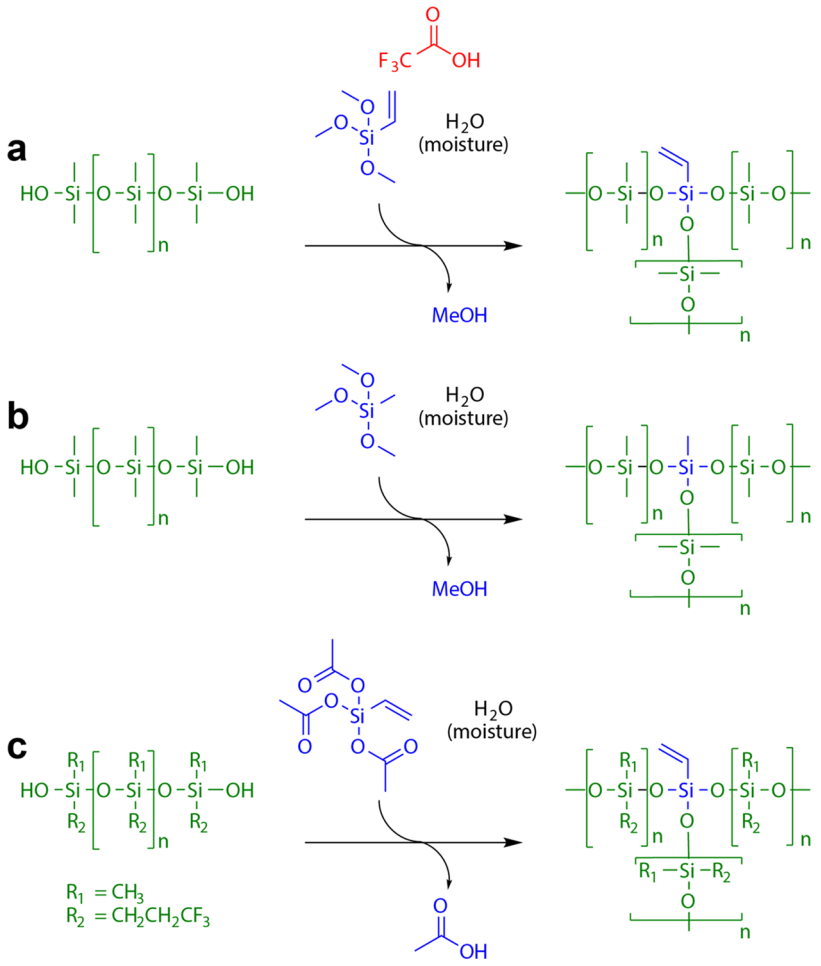

Figure 1. Moisture-activated curing of silicones. (a) **Silicone 1**; (b) **Silicone 2**; (c) **Fluorosilicone 1**. The compounds shown in green, blue, and red are polymer chains, crosslinkers, and catalysts, respectively.

exposure to moisture in the air (Figure 1). The precursor of **Silicone 2** contains hydroxy-terminated poly(dimethylsiloxane) (PDMS−OH), methyltrimethoxysilane (crosslinker), a titanium catalyst,[25] and silica filler treated with hexamethyldisilazane. When the crosslinker is mixed with PDMS−OH, the Si−OH functional groups react with the crosslinker, releasing methanol and producing crosslinker-terminated PDMS chains.[46] Upon exposure to humid air, some of the methoxy groups of the still unreacted crosslinker and the crosslinker-terminated PDMS are hydrolyzed, releasing more methanol and producing additional Si−OH functional groups, which then react with Si−OH or Si−OMe groups to form a crosslinked polymer. **Fluorosilicone 1** is an acetic acid-evolving fluorosilicone that cures in a similar manner as **Silicone 2**. It contains hydroxy-terminated poly(trifluoropropylmethyl)siloxane, a silica filler (treated with hexamethyldisilazane), and vinyltriacetoxysilane as a crosslinker. Upon exposure to moisture, acetate groups are hydrolyzed, releasing acetic acid, which further catalyzes crosslinking.

Although these commercial silicones are attractive candidates for use in plasticizer-free ion-selective electrodes, the complete composition of their precursor formulations is not public information. This makes it challenging to understand how the ISE response characteristics are affected by the silicone composition and what species remain in the silicone matrix upon curing.[18] To compare ISEs prepared with **Silicone 2** and **Fluorosilicone 1** to a silicone of known composition, we prepared our own PDMS with no added fillers and with reagents that can be removed by evaporation after curing, adapting a reported procedure (see the Supporting Information, Section S1.2 and Table S1 for details on curing).[47]

Response Characteristics of K^+ SC-ISEs Prepared with Silicones and CIM Carbon. Solid-contact K^+ ISEs were prepared with **Silicone 1**, **Silicone 2**, or **Fluorosilicone 1** as the ion-selective membrane matrix, valinomycin as ionophore, KTpClPB to provide ionic sites, CIM carbon as the solid contact, and graphite rods encased in glass bodies as the contacting electron conductor (Figure S1c−e). After initial conditioning in 1 mM KCl at 25 °C for 22 h, all three types of SC-ISEs exhibited Nernstian responses to K^+, excellent selectivity to K^+ versus Na^+, and micromolar detection limits (Figure 2 and Table 1). No changes in response characteristics (measured at 25 °C) were observed after storage in 1 mM KCl solution at 37 °C for 18 days (see Table 1 and Figure S3). All three types of SC-ISEs were also insensitive to oxygen (Figure S18), consistent with PVC-based ISEs prepared with CIM carbon as the solid contact.[45] Interestingly, there is no significant difference in selectivities for these ISEs and ISEs with membranes prepared with PVC (plasticized with DOS), silicone, or fluorosilicone membranes as reported in the literature.[45,48,49]

Long-Term Stability of K^+ SC-ISEs. For wearable and implantable applications, it is important to know how often the

https://doi.org/10.1021/acs.analchem.3c02074
Anal. Chem. 2023, 95, 12419−12426

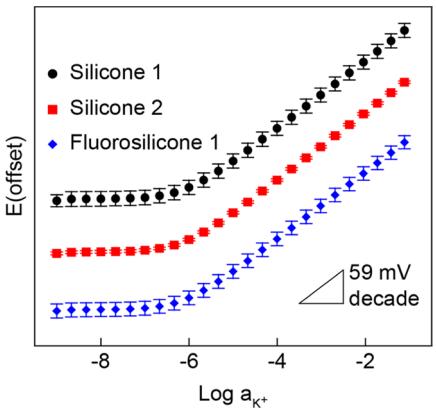

Figure 2. Potentiometric response curves of solid-contact K^+ ISEs (**Batch 1**) prepared with **Silicone 1**, **Silicone 2**, or **Fluorosilicone 1** as polymeric matrix after conditioning in 1 mM KCl at 25 °C for 23 h. Symbols represent average potentials for four identically prepared ISEs, and error bars represent standard deviations. See Figure S2 for responses of individual ISEs.

sensors need to be recalibrated.[50] To understand these characteristics, the potentials of the K^+ SC-ISEs (**Batch 1**) were measured during initial conditioning at 25 °C for 23 h relative to a double-junction Ag/AgCl reference electrode (Figure S7). SC-ISEs prepared with **Silicone 2** and **Fluorosilicone 1** exhibited a large increase in potential in the first 3 h, followed by a smaller drift toward higher and lower potentials, respectively, whereas SC-ISEs prepared with **Silicone 1** showed only a small drift toward higher potential throughout the entire measurement. Noting that the added ionic site salt comprised the primary ion, the large initial changes in potential are likely caused by water uptake into the ISE membranes[42] and leaching of hydrophilic ionic and uncharged impurities from the membranes into the aqueous solution.

Further conditioning of the SC-ISEs in 1 mM KCl at the physiological temperature (37 °C) revealed that SC-ISEs prepared with all types of silicones tested can reach very low potential drift values (Figure 3). The **Silicone 1** and **Fluorosilicone 1** membranes exhibited average drifts of 9 ± 6 and 3 ± 6 μV/h, respectively, values that are comparable to those of PVC-based SC-ISEs prepared with CIM carbon[45] and 3DOM carbon.[51] The drift for **Silicone** 2 SC-ISEs (27 ± 18 μV/h) did not differ significantly (95% confidence limit) from those for **Silicone 1** and **Fluorosilicone 1**. The same is true for the ISEs prepared in **Batch 2** (see Figure S8 and Table S3).

Performance of K^+ ISEs upon Exposure to Porcine Blood Plasma. To test the sensor behavior in clinically relevant samples, we chose porcine plasma as a model system because it contains all of the relevant chemical species (interfering ions, proteins, lipids, and organic compounds) one would expect to encounter in wearable or implantable applications. Additionally, blood plasma does not contain red blood cells, which simplifies the system and eliminates complications caused by the leaching of K^+ from the blood cells into the plasma, but it means that any possible effects of red blood cells on the ISEs are neglected. K^+ activities and concentrations were measured in porcine plasma and compared to the values determined by ion chromatography (Table 2). A three-point calibration curve was used to calculate the K^+ activity from the measured ISE potential (**Batch 1**) in porcine plasma (Figure S10), with all data corrected in the usual manner for the liquid junction potential and activity coefficients. The potentials measured in porcine plasma were corrected for the liquid junction potential using Bjerrum's method (see Supporting Information, Section S1.8 and Figure S11).

The activity of K^+ in porcine plasma measured with the SC-ISEs is lower than the concentration determined by ion chromatography (Table 2), which is expected since the ionic strength of blood is ∼150 mM. To compare the two values, the activity coefficient for K^+ in blood plasma was estimated using the extended Debye−Hückel equation. Approximating the plasma as a solution with 150 mM ionic strength, the activity coefficient for K^+ in blood plasma is 0.73.[52] Using the K^+ concentration in the porcine plasma from ion chromatography, the expected activity of K^+ in the porcine plasma is 7.4 ± 0.1 mM, which is in agreement with the results from the **Silicone 2**-based SC-ISEs (7.6 ± 0.4 mM). The measured K^+ activity from the **Silicone 1**- and **Fluorosilicone 1**-based SC-ISEs was 8.1 ± 0.5 and 5.5 ± 0.5 mM, respectively. Notably, upon exposure to porcine plasma, the **Fluorosilicone 1**-based ISEs exhibited a quick step change toward lower potential, followed by a large drift toward lower potential (Figure S10d). **Silicone 1**- and **Silicone 2**-based ISEs did not have the same large step change upon exposure to porcine plasma. Using a Student's *t*-test assuming unpaired data with unequal variances, the difference between ion chromatography values and those obtained using **Silicone 1**- or **Fluorosilicone 1**-based SC-ISEs is statistically significant even at the 99% confidence limit.

To better understand the ISE performance in blood plasma, measurements were also performed with the method of standard addition, making it possible to determine the K^+ concentration (rather than the activity). With 95% certainty,

Table 1. Response Characteristics of Silicone 1-, Silicone 2-, and Fluorosilicone 1-Based SC-ISEs (Batch 1) after Conditioning in 1 mM KCl Solution

polymer matrix	response slope[a] (mV/decade) after 23 h at 25 °C	response slope[a] (mV/decade) after 433 h at 37 °C	log K_{K^+,Na^+} after 23 h[b] at 25 °C	log K_{K^+,Na^+} after 433 h[b] at 37 °C	drift (25 °C)[c,d] (μV/h)	drift (37 °C)[e,f] (μV/h)
Silicone 1	60.0 ± 0.1	59.4 ± 0.1	−4.52 ± 0.08	−4.56 ± 0.04	336 ± 111	9 ± 6
Silicone 2	59.9 ± 0.1	59.5 ± 0.1	−4.60 ± 0.01	−4.58 ± 0.01	216 ± 38	27 ± 18
Fluorosilicone 1	59.1 ± 0.1	59.0 ± 0.1	−4.70 ± 0.02	−4.49 ± 0.05	308 ± 264	3 ± 6

[a]Response slopes were measured at 25 °C even though the temperature during conditioning was 37 °C. [b]Selectivity was measured by the fixed interference method at 25 °C. [c]Drift calculated by linear fit of potentials measured during 25 °C stability experiment from 18 to 23 h. [d]Potential measured relative to a double-junction Ag/AgCl reference electrode with a 1 M lithium acetate salt bridge. [e]Drift calculated by linear fit of potentials measured during 37 °C stability experiment from 20 to 143 h. [f]ISE potentials referenced to a Ag/AgCl wire placed in the sample solution.

https://doi.org/10.1021/acs.analchem.3c02074
Anal. Chem. 2023, 95, 12419−12426

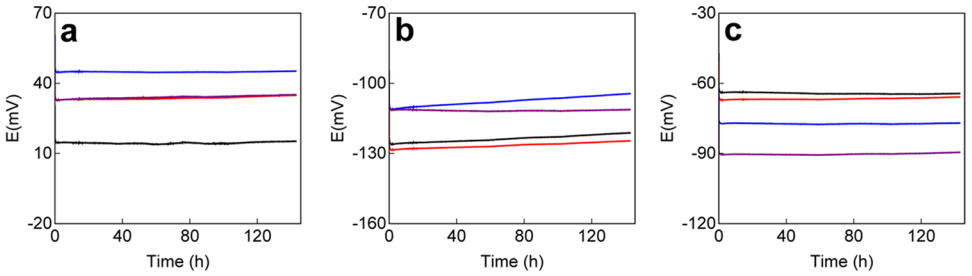

Figure 3. Response of K^+ SC-ISEs (**Batch 1**) with conditioning in 1 mM KCl solution at 37 °C relative to a Ag/AgCl wire (a) **Silicone 1**, (b) **Silicone 2**, (c) **Fluorosilicone 1**. Shown in each graph are potentials for four identically prepared ISEs. See the Supporting Information for the prior history of these electrodes.

Table 2. Measured K^+ Activity and Concentration in Porcine Blood Plasma Using SC-ISEs from Batch 1[a]

silicone or measurement technique	K^+ activity in porcine plasma (mM)	K^+ concentration in porcine plasma (mM)[b]
Silicone 1	8.1 ± 0.5 (n = 16)[c]	10.9 ± 0.3 (n = 4)
Silicone 2	7.6 ± 0.4 (n = 16)[c]	11.1 ± 0.1 (n = 4)
Fluorosilicone 1	5.5 ± 0.5 (n = 16)[c]	11.8 ± 0.4 (n = 4)
ion chromatography	7.4 ± 0.1 (n = 11)[d]	10.2 ± 0.1 (n = 11)[e]

[a]Values are reported as average ± standard deviation. [b]The K^+ concentration was measured with the method of standard addition. [c]The K^+ activity was measured four times with each ISE, resulting in 16 total measurements (see Supporting Information, Section S1.7 for more information). [d]The K^+ activity was calculated from the K^+ concentration measured by ion chromatography using the extended Debye−Hückel equation, considering the blood plasma as a solution with an ionic strength of 150 mM. [e]This K^+ concentration is well above the expected concentration in porcine plasma (4.4−6.7 mM),[53] likely because some red blood cells burst during collection, storage, or handling of the blood, which is known to raise the K^+ concentration in plasma.

the K^+ concentrations measured using SC-ISEs prepared with **Silicone 1** and **Silicone 2** were higher than the value measured by ion chromatography. The slightly higher than expected concentrations can be explained by the drifts toward the lower potential observed in this experiment (Figure S12g,h). For SC-ISEs prepared with **Fluorosilicone 1**, the measured K^+ concentration was significantly higher than the values obtained using ISEs prepared with **Silicone 1** and **Silicone 2** (the differences are statistically significant at the 95% confidence limit). Notably, even though the K^+ concentration and activity as determined with the **Fluorosilicone 1** ISEs differs from the value measured by ion chromatography, the sensors still have Nernstian responses to changes in K^+ concentration in blood plasma (Figure S12f). Evidently, the process that causes the potential of the **Fluorosilicone 1** SC-ISEs to decrease in blood plasma does not affect the selectivity of the sensor during short-term exposures. So long as the sensor responds to K^+ and the EMF offset in blood plasma is constant during the method of standard addition experiment, the EMF offset will not affect the value of the measured K^+ concentration.

Performance of ISEs during Long-Term Exposure to Porcine Plasma at 37 °C. The stability of the ISEs in porcine plasma was measured at 37 °C over a period of 41 h (see Figure 4 and Table 3). The **Silicone 1**-based ISEs (Figure 4a) had a large, continuous drift toward lower potential during the 41 h exposure to porcine plasma, whereas ISEs prepared with **Silicone 2** (Figure 4b) had a much smaller drift (−55 ± 51 μV/h) after an initial decrease in potential within the 1st hour. The difference in drift between SC-ISEs prepared with different silicone membranes was consistent between two different batches of ISEs (see Figure S9 and Table S3).

As the **Silicone 1** SC-ISE, the **Fluorosilicone 1** SC-ISEs too had a large drift toward lower potential, but the drift decreased with increasing exposure time to porcine plasma. The magnitude of the drift (30−41 h) for the **Fluorosilicone 1** SC-ISEs is 297 μV/h, which is larger than the reported drift of 85 ± 15 μV/h in whole blood using a sensor prepared with a plasticized **Fluorosilicone 1** (10.5% DOS) membrane coated onto a Ag electrode.[43] However, in that report, a stop-flow setup was used, and the ISEs were only exposed to blood for ∼10 min at a time before being washed with KCl solutions.

After exposure to porcine plasma for 41 h at 37 °C, the response and selectivity of the K^+ ISEs were measured again at 25 °C (Table 3, see the Supporting Information, Sections S1.5 and S1.9 for experimental details). ISEs prepared with all silicones and the fluorosilicone maintained a Nernstian response to K^+ (Figure S6). Although the selectivity worsened

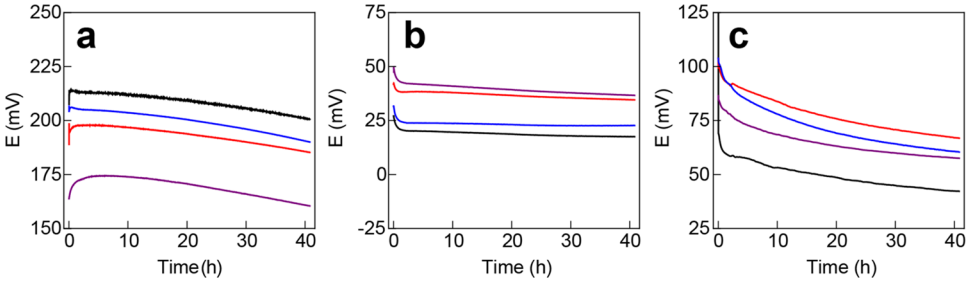

Figure 4. Long-term potential stability of solid-contact K^+ ISEs (**Batch 2**) in porcine plasma at 37 °C for ISEs prepared with (a) **Silicone 1**, (b) **Silicone 2**, and (c) **Fluorosilicone 1**. Shown in each graph are potentials for four identically prepared ISEs measured at the same time, in the same solution, relative to a Ag/AgCl double-junction reference electrode with a 1 M lithium acetate outer filling solution.

https://doi.org/10.1021/acs.analchem.3c02074
Anal. Chem. 2023, 95, 12419−12426

Table 3. Stability and Response Characteristics of SC-ISEs (Batch 2) during and after Exposure to Porcine Plasma at 37 °C for 41 h

silicone	drift[a] (μV/h)	response slope[b] (mV/decade)	detection limit[c] (μM)	selectivity[d] ($\log K_{K^+,Na^+}$)
Silicone 1	−495 ± 50	62.7 ± 0.4	1.6 ± 0.2	−4.04 ± 0.07
Silicone 2	−55 ± 51	62.1 ± 0.4	1.9 ± 0.1	−4.00 ± 0.02
Fluorosilicone 2	−297 ± 69	62.1 ± 0.4	2.4 ± 0.2	−3.90 ± 0.02

[a]Drifts were measured relative to a double-junction reference electrode at 37 °C for 41 h and calculated as a linear fit of potentials from 30 to 41 h. [b]Response slopes were calculated from a calibration curve at 25 °C in the range of 10^{-4}–10^{-1} M KCl, collected immediately after the 41 h exposure to porcine plasma at 37 °C. [c]Detection limits were obtained from a calibration curve collected immediately after exposure to porcine plasma for 41 h. [d]FIM selectivity measurements were conducted immediately after the calibration curve outlined in footnote b.

slightly, it was still high enough for use in physiological samples. This effect might be caused by the extraction of neutral hydrophobic species, such as lipids, from the blood plasma.[54] Uptake of such species into the membrane could also be responsible for the observed sensor drift in blood plasma, raising the question whether conditioning of new sensors in plasma could reduce subsequent drift and improve the accuracy of measurements. Interestingly, the selectivity of SC-ISEs that had been stored in 1 mM KCl solution for 17 days after a 39 h exposure to blood plasma (**Batch 1**) was the same as before long-term exposure to porcine plasma (Table S3), suggesting that the effect of porcine plasma exposure on the selectivity is reversible.

To explore whether there are any differences in their membrane structure, **Silicone 1** and **Silicone 2** were analyzed by ATR-FTIR (Figure S13) and differential scanning calorimetry (DSC; see Figures S15 and S16). However, no notable differences between the two silicones were observed. The DSC data for **Silicone 1** and **Silicone 2** are typical for silicones; both had a low glass-transition temperature of −118 °C and peaks corresponding to melting at −45 °C and crystallization between −73 and −75 °C. The ATR-FTIR spectra are also consistent with the structure of silicones. **Silicone 2** contains a peak at 470 cm^{-1} that likely corresponds to symmetric Si−O−Si bending modes from the silica filler in **Silicone 2**.[55] This peak is not present in **Silicone 1**, but it can also be found in the FTIR spectrum of **Fluorosilicone 1** (Figure S14), which also contains silica filler. It is unclear whether the filler affects the drift of these sensors in blood plasma or whether there are other more important structural features not readily detected by FTIR or evident from DSC. For example, membranes prepared with **Silicone 2** (100 ± 50 and 3 ± 1 GΩ·cm for undoped and doped membranes, respectively) have a much lower resistivity than membranes prepared with **Silicone 1** (200 ± 100 and 40 ± 30 GΩ·cm for undoped and doped membranes, respectively, measured with the known shunt method, see Table S2), which might be caused by a lower crosslink density of **Silicone 2** compared to **Silicone 1**; ions are expected to have a lower mobility in a more crosslinked polymer.

CONCLUSIONS

With this work, we show that SC-ISEs prepared with plasticizer-free silicone or fluorosilicone membranes and CIM carbon as the solid contact have Nernstian response slopes, excellent selectivity, and as far as we know, the lowest potential drifts reported so far for SC-ISEs with silicone membranes in aqueous salt solutions. Of the reports in the literature on silicone-based ISEs, only a few contain quantitative data for long-term stability (Table S4). The drift of K^+ SC-ISEs prepared in this work with **Silicone 2** and CIM carbon as solid contact in aqueous salt solutions (7 ± 5 μV/h) is much lower than the reported value for a Ca^{2+} SC-ISE prepared with a silicone ISM and graphene/polyaniline solid contact (200 μV/h),[56] though differences in conditioning time and sample temperature may contribute to the difference in drift. The authors of that paper also mentioned the possible dissolution of polyaniline into the ISM, which may have also contributed to drift, whereas ISEs prepared with CIM carbon do not suffer from such a problem. The drift of SC-ISEs prepared with **Fluorosilicone 1** (3 ± 5 μV/h) and CIM carbon as the solid contact is also lower than that reported for a K^+ ISE prepared with plasticized (DOS) **Fluorosilicone 1** (10 μV/h) on a Ag electrode.[43]

This work also shows that small differences in silicone composition can have a large influence on the long-term stability of SC-ISEs, especially in complex samples. In blood plasma, SC-ISEs prepared with **Silicone 2** exhibited a drift of −55 ± 51 μV/h, much lower than ISEs prepared with **Silicone 1** (−495 ± 50 μV/h) and **Fluorosilicone 1** (−297 ± 69 μV/h). Although the structures of **Silicone 1** and **Silicone 2** are nominally the same, the difference in drift is large. The cause of this difference is not well understood and will be the subject of future study. The recent literature has emphasized the importance of minimizing long-term drifts of SC-ISEs, and typically those drifts are measured in electrolyte solutions. The example here shows that drift in aqueous solution does not necessarily correlate to drift in real samples, emphasizing the importance of drift measurements in samples for which the sensors are developed.

ASSOCIATED CONTENT

Supporting Information

The Supporting Information is available free of charge at https://pubs.acs.org/doi/10.1021/acs.analchem.3c02074.

Details regarding CIM carbon synthesis and procedures for electrode fabrication, calibration and selectivity measurements, K^+ activity and concentration measurements in porcine plasma, estimation of the liquid junction potential, calibration curves for individual SC-ISEs in KCl and blood plasma, and DSC and ATR-FTIR analysis of the silicone and fluorosilicone membranes (PDF)

AUTHOR INFORMATION

Corresponding Authors

Philippe Bühlmann − *Department of Chemistry, University of Minnesota, Minneapolis, Minnesota 55454, United States;* orcid.org/0000-0001-9302-4674; Email: buhlmann@umn.edu

https://doi.org/10.1021/acs.analchem.3c02074
Anal. Chem. 2023, 95, 12419−12426

Andreas Stein − *Department of Chemistry, University of Minnesota, Minneapolis, Minnesota 55454, United States;* orcid.org/0000-0001-8576-0727; Email: a-stein@umn.edu

Authors

Brian D. Spindler − *Department of Chemistry, University of Minnesota, Minneapolis, Minnesota 55454, United States*

Katerina I. Graf − *Department of Chemistry, University of Minnesota, Minneapolis, Minnesota 55454, United States*

Xin I. N. Dong − *Department of Chemistry, University of Minnesota, Minneapolis, Minnesota 55454, United States*

Minog Kim − *Department of Chemistry, University of Minnesota, Minneapolis, Minnesota 55454, United States;* orcid.org/0000-0001-7963-1734

Xin V. Chen − *Department of Chemistry, University of Minnesota, Minneapolis, Minnesota 55454, United States;* orcid.org/0000-0003-4477-043X

Complete contact information is available at: https://pubs.acs.org/10.1021/acs.analchem.3c02074

Notes

The authors declare the following competing financial interest(s): This work was funded in part by Medtronic PLC. A.S., P.B., and the University of Minnesota (UMN) have a patent and a patent application (U.S. patent no. 9,874,539; US2020/059979) relating to the use of CIM carbon in ion-selective and reference electrodes. The UMN and the inventors are entitled to standard royalties should licensing revenue be generated from these inventions.

■ ACKNOWLEDGMENTS

Portions of this work were supported by Medtronic. Parts of this work were carried out in the University of Minnesota Characterization Facility, which receives partial support from the NSF through the MRSEC (Award Number DMR-2011401) and the NNCI (Award Number ECCS2025124) programs.

■ REFERENCES

(1) Lewenstam, A. *Electroanalysis* **2014**, *26*, 1171−1181.
(2) Crespo, G. A. *Electrochim. Acta* **2017**, *245*, 1023−1034.
(3) Bakker, E. *TrAc, Trends Anal. Chem.* **2014**, *53*, 98−105.
(4) Michalska, A. *Anal. Bioanal. Chem.* **2006**, *384*, 391−406.
(5) Bakker, E.; Bühlmann, P.; Pretsch, E. *Chem. Rev.* **1997**, *97*, 3083−3132.
(6) Bühlmann, P.; Pretsch, E.; Bakker, E. *Chem. Rev.* **1998**, *98*, 1593−1688.
(7) Gao, W.; Emaminejad, S.; Nyein, H. Y.; Challa, S.; Chen, K.; Peck, A.; Fahad, H. M.; Ota, H.; Shiraki, H.; Kiriya, D.; Lien, D. H.; Brooks, G. A.; Davis, R. W.; Javey, A. *Nature* **2016**, *529*, 509−514.
(8) Parrilla, M.; Cuartero, M.; Padrell Sánchez, S.; Rajabi, M.; Roxhed, N.; Niklaus, F.; Crespo, G. A. *Anal. Chem.* **2019**, *91*, 1578−1586.
(9) Parrilla, M.; Ortiz-Gómez, I.; Cánovas, R.; Salinas-Castillo, A.; Cuartero, M.; Crespo, G. A. *Anal. Chem.* **2019**, *91*, 8644−8651.
(10) Cao, Q.; Liang, B.; Mao, X.; Wei, J.; Tu, T.; Fang, L.; Ye, X. *Electroanalysis* **2021**, *33*, 643−651.
(11) Roy, S.; David-Pur, M.; Hanein, Y. *ACS Appl. Mater. Interfaces* **2017**, *9*, 35169−35177.
(12) Parrilla, M.; Cuartero, M.; Crespo, G. A. *TrAC, Trends Anal. Chem.* **2019**, *110*, 303−320.
(13) Bandodkar, A. J.; Hung, V. W.; Jia, W.; Valdes-Ramirez, G.; Windmiller, J. R.; Martinez, A. G.; Ramirez, J.; Chan, G.; Kerman, K.; Wang, J. *Analyst* **2013**, *138*, 123−128.
(14) Zhu, D. D.; Tan, Y. R.; Zheng, L. W.; Lao, J. Z.; Liu, J. Y.; Yu, J.; Chen, P. *ACS Appl. Mater. Interfaces* **2023**, *15*, 14146−14154.
(15) Cosofret, V. V.; Erdösy, M.; Buck, R. P.; Kao, W. J.; Anderson, J. M.; Lindner, E.; Neuman, M. R. *Analyst* **1994**, *119*, 2283−2292.
(16) Gourlay, T.; Samartzis, I.; Stefanou, D.; Taylor, K. *Artif. Organs* **2003**, *27*, 256−260.
(17) Dinten, O.; Spichiger, U. E.; Chaniotakis, N.; Gehrig, P.; Rusterholz, B.; Morf, W. E.; Simon, W. *Anal. Chem.* **1991**, *63*, 596−603.
(18) Chen, X. V.; Bühlmann, P. *Curr. Opin. Electrochem.* **2022**, *32*, No. 100896.
(19) Anderson, E. L.; Chopade, S. A.; Spindler, B. D.; Stein, A.; Lodge, T. P.; Hillmyer, M. A.; Bühlmann, P. *Anal. Chem.* **2020**, *92*, 7621−7629.
(20) Heng, L. Y.; Hall, E. A. H. *Anal. Chim. Acta* **2000**, *403*, 77−89.
(21) Uhlig, A.; Lindner, E.; Teutloff, C.; Schnakenberg, U.; Hintsche, R. *Anal. Chem.* **1997**, *69*, 4032−4038.
(22) Curtis, J.; Colas, A. Medical Applications of Silicones. In *Biomaterial Science*, 3rd ed.; Ratner, B. D.; Hoffman, A. S.; Schoen, F. J.; Lemons, J. E., Eds.; Academic Press, 2013; pp 1106−1116.
(23) Fogt, E. J.; Untereker, D. F.; Norenberg, M. S.; Meyerhoff, M. E. *Anal. Chem.* **1985**, *57*, 1995−1998.
(24) Sudhölter, E. J.; van der Wal, P. D.; Skowronska-Ptasinska, M.; van den Berg, A.; Bergveld, P.; Reinhoudt, D. N. *Anal. Chim. Acta* **1990**, *230*, 59−65.
(25) van der Wal, P. D.; Skowronska-Ptasinska, M.; van den Berg, A.; Bergveld, P.; Sudhölter, E. J. R.; Reinhoudt, D. N. *Anal. Chim. Acta* **1990**, *231*, 41−52.
(26) Kimura, K.; Matsuba, T.; Tsujimura, Y.; Yokoyama, M. *Anal. Chem.* **1992**, *64*, 2508−2511.
(27) Tsujimura, Y.; Yokoyama, M.; Kimura, K. *Electroanalysis* **1993**, *5*, 803−807.
(28) Reinhoudt, D. N.; Engbersen, J. F. J.; Brzozka, Z.; van der Vlekkert, H. H.; Honig, G. W. N.; Holterman, H. A. J.; Verkerk, U. H. *Anal. Chem.* **1994**, *66*, 3618−3623.
(29) Tsujimura, Y.; Yokoyama, M.; Kimura, K. *Sens. Actuators, B* **1994**, *22*, 195−199.
(30) Poplawski, M. E.; Brown, R. B.; Lae Rho, K.; Yong Yun, S.; Jung Lee, H.; Sig Cha, G.; Paeng, K.-J. *Anal. Chim. Acta* **1997**, *355*, 249−257.
(31) Szűcs, J.; Lindfors, T.; Bobacka, J.; Gyurcsányi, R. E. *Electroanalysis* **2016**, *28*, 778−786.
(32) Lindfors, T.; Szűcs, J.; Sundfors, F.; Gyurcsanyi, R. E. *Anal. Chem.* **2010**, *82*, 9425−9432.
(33) Knoll, M.; Cammann, K.; Dumschat, C.; Sundermeier, C.; Eshold, J. *Sens. Actuators, B* **1994**, *18*, 51−55.
(34) Shin, J. H.; Lee, H. J.; Kim, C. Y.; Oh, B. K.; Rho, K. L.; Nam, H.; Cha, G. S. *Anal. Chem.* **1996**, *68*, 3166−3172.
(35) Oh, B. K.; Kim, C. Y.; Lee, H. J.; Rho, K. L.; Cha, G. S.; Nam, H. *Anal. Chem.* **1996**, *68*, 503−508.
(36) van der Wal, P. D.; Sudhölter, E. J. R.; Reinhoudt, D. N. *Anal. Chim. Acta* **1991**, *245*, 159−166.
(37) van der Wal, P. D.; Sudhölter, E. J. R.; Boukamp, B. A.; Bouwmeester, H. J. M.; Reinhoudt, D. N. *J. Electroanal. Chem. Interfacial Electrochem.* **1991**, *317*, 153−168.
(38) Brunink, J. A. J.; Lugtenberg, R. J. W.; Brzøzka, Z.; Engbersen, J. F. J.; Reinhoudt, D. N. *J. Electroanal. Chem.* **1994**, *378*, 185−200.
(39) Högg, G.; Lutze, O.; Cammann, K. *Anal. Chim. Acta* **1996**, *335*, 103−109.
(40) Cazalé, A.; Sant, W.; Launay, J.; Ginot, F.; Temple-Boyer, P. *Sens. Actuators, B* **2013**, *177*, 515−521.
(41) Pick, J.; Tóth, K.; Pungor, E.; Vasák, M.; Simson, W. *Anal. Chim. Acta* **1973**, *64*, 477−480.
(42) Lindfors, T.; Höfler, L.; Jágerszki, G.; Gyurcsányi, R. E. *Anal. Chem.* **2011**, *83*, 4902−4908.
(43) Scheipers, A.; Waßmus, O.; Sundermeier, C.; Eshold, J.; Weiß, T.; Gitter, M.; Roß, B.; Knoll, M. *Anal. Chim. Acta* **2001**, *439*, 29−38.
(44) Yajima, S.; Kishi, M.; Kimura, K. *Bunseki Kagaku* **2017**, *66*, 431−436.

(45) Hu, J.; Zou, X. U.; Stein, A.; Bühlmann, P. *Anal. Chem.* **2014**, *86*, 7111−7118.
(46) Thomas, D. R. *Cross-Linking of Polydimethylsiloxanes*; PTR Prentice Hall: Englewood Cliffs, NJ, 1993.
(47) Mincheva, R.; Beigbeder, A.; Pettitt, M. E.; Callow, M. E.; Callow, J. A.; Dubois, P. *Nanocomposites* **2016**, *2*, 51−57.
(48) Bakker, E. *J. Electrochem. Soc.* **1996**, *143*, L83−L85.
(49) Yoon, I. J.; Lee, D. K.; Nam, H.; Cha, G. S.; Strong, T. D.; Brown, R. B. *J. Electroanal. Chem.* **1999**, *464*, 135−142.
(50) Rousseau, C. R.; Bühlmann, P. *TrAC, Trends Anal. Chem.* **2021**, *140*, No. 116277.
(51) Lai, C. Z.; Fierke, M. A.; Stein, A.; Bühlmann, P. *Anal. Chem.* **2007**, *79*, 4621−4626.
(52) Covington, A. K.; Robinson, R. A. *Anal. Chim. Acta* **1975**, *78*, 219−223.
(53) Carlson, G. P.; Bruss, M. Fluid, Electrolyte, and Acid-Base Balance. In *Clinical Biochemistry of Domestic Animals*, 6th ed.; Kaneko, J. J.; Harvey, J. W.; Bruss, M. L., Eds.; Academic Press: San Diego, 2008; Chapter 17, pp 529−559.
(54) Bühlmann, P.; Hayakawa, M.; Ohshiro, T.; Amemiya, S.; Umezawa, Y. *Anal. Chem.* **2001**, *73*, 3199−3205.
(55) Lippincott, E. R.; Valkenburg, A. V.; Weir, C. E.; Bunting, E. N. *J. Res. Natl. Bur. Stand.* **1958**, *61*, 61−70.
(56) Boeva, Z. A.; Lindfors, T. *Sens. Actuators, B* **2016**, *224*, 624−631.

https://doi.org/10.1021/acs.analchem.3c02074
Anal. Chem. 2023, 95, 12419−12426